Analytic solutions for three dimensional swirling strength in compressible and incompressible flows

Huai Chen, Ronald J. Adrian, Qiang Zhong, and Xingkui Wang

Citation: Physics of Fluids (1994-present) **26**, 081701 (2014); doi: 10.1063/1.4893343
View online: http://dx.doi.org/10.1063/1.4893343
View Table of Contents: http://scitation.aip.org/content/aip/journal/pof2/26/8?ver=pdfcov
Published by the AIP Publishing

PHYSICS OF FLUIDS **26**, 081701 (2014)

Analytic solutions for three dimensional swirling strength in compressible and incompressible flows

Huai Chen,[1] Ronald J. Adrian,[2,a)] Qiang Zhong,[1] and Xingkui Wang[1]
[1]*State Key Laboratory of Hydroscience and Engineering, Tsinghua University, Beijing 100084, China*
[2]*School for Engineering Matter, Transport and Energy, Arizona State University, Tempe, Arizona 85287, USA*

(Received 27 April 2014; accepted 27 July 2014; published online 20 August 2014)

Eigenvalues of the 3D critical point equation $(\nabla \mathbf{u})v = \lambda v$ are normally computed numerically. In the letter, we present analytic solutions for 3D swirling strength in both compressible and incompressible flows. The solutions expose functional dependencies that cannot be seen in numerical solutions. To illustrate, we study the difference between using fluctuating and total velocity gradient tensors for vortex identification. Results show that mean shear influences vortex detection and that distortion can occur, depending on the strength of mean shear relative to the vorticity at the vortex center. © *2014 AIP Publishing LLC*. [http://dx.doi.org/10.1063/1.4893343]

There are a number of point-wise vortex identification techniques based on the velocity gradient tensor. These include the second invariant of velocity gradient tensor,[1] the discriminant of the velocity gradient tensor,[2] the Hessian of pressure,[3] and the swirling strength method.[4] The swirling strength method uses the imaginary part of the complex eigenvalue of the velocity gradient tensor to visualize vortices.

Let $A_{mn} = \partial u_m/\partial x_n$ (m, n = 1,2,3) be the velocity gradient tensor $\mathbf{A}(\mathbf{x}) = \nabla \mathbf{u}$ of 3D flow at a point, $\mathbf{x}$. The eigenvalue problem $\mathbf{A}v_\alpha = \lambda_\alpha v_\alpha$ has three eigenvalues λ_α and three corresponding eigenvectors v_α, $\alpha = 1, 2, 3$. Local motion around the critical point exhibits swirling (rotation) if the eigenvalues of $\boldsymbol{A}$ are complex.[2] In this case, the gradient tensor can be decomposed as[4]

$$\boldsymbol{A} = [\vec{v}_r \vec{v}_{cr} \vec{v}_{ci}] \begin{bmatrix} \lambda_r & 0 & 0 \\ 0 & \lambda_{cr} & \lambda_{ci} \\ 0 & -\lambda_{ci} & \lambda_{cr} \end{bmatrix} [\vec{v}_r \vec{v}_{cr} \vec{v}_{ci}]^{-1}, \tag{1}$$

where λ_r is the real eigenvalue with a corresponding eigenvector, v_r and $\lambda_{cr} \pm i\lambda_{ci}$ are the conjugate pair of the complex eigenvalues with complex eigenvectors $v_{cr} \pm iv_{ci}$. The advantage of the swirling strength concept is its simple physical meaning as the frequency at which fluid particles swirl around the critical point.[4]

Universally, until now, λ_{ci} has been evaluated in 3D flow point-wise by solving the eigenvalue problem, numerically. While the decomposition of $\boldsymbol{A}$ is easily done numerically, numerical solution does not provide insight into the parametric dependencies of swirling strength. Here, we present an exact algebraic solution for λ_{ci}, in both incompressible and compressible flows, whose value lies in (1) reducing computation; and (2) providing a basis for further analysis of its properties.

The characteristic equation of the velocity gradient tensor $\boldsymbol{A}$ is given by

$$\lambda^3 + P\lambda^2 + Q\lambda + R = 0, \tag{2}$$

where $P = -\mathrm{tr}(\boldsymbol{A})$, $Q = 0.5\mathrm{tr}(P^2\text{-}\boldsymbol{AA})$ and $R = -\det(\boldsymbol{A})$. We solve this equation using Cardano's method.[5] Let $t = \lambda\text{-}P/3$, $p = Q\text{-}P^2/3$, and $q = R\text{-}PQ/3\text{-}2P^3/27$ to get the simpler equation

$$t^3 + pt + q = 0. \tag{3}$$

a)Electronic mail: rjadrian@asu.edu

Putting $t = \zeta + \eta$ and setting $\zeta\eta = -p/3$ yields a quadratic equation in ζ^3,

$$(\zeta^3)^2 + q(\zeta^3) - p^3/27 = 0. \tag{4}$$

It is easy to solve (4) by the quadratic formula, and as a result of symmetry between ζ and η, we can set $\zeta^3 = -q/2 + sqrt(\Delta)$ and $\eta^3 = -q/2\text{-}sqrt(\Delta)$, where $\Delta = (q/2)^2 + (p/3)^3$ is the discriminant. When Δ is positive, Eq. (2) has a real eigenvalue and a conjugate pair of complex eigenvalues:

$$\begin{cases} \lambda_1 = \zeta + \eta + P/3 \\ \lambda_2 = \beta\zeta + \beta^2\eta = -(\zeta+\eta)/2 + P/3 + i\sqrt{3}(\zeta-\eta)/2 \\ \lambda_3 = \beta^2\zeta + \beta\eta = -(\zeta+\eta)/2 + P/3 - i\sqrt{3}(\zeta-\eta)/2 \end{cases}, \tag{5}$$

where β is the primitive cube root of unity. In accordance with Eq. (1), $\lambda_r = \zeta + \eta + P/3$, $\lambda_{cr} = -(\zeta+\eta)/2 + P/3$, $\lambda_{ci} = \sqrt{3}(\zeta-\eta)/2$. It is easy to prove that $\forall\zeta, \eta \in R$, $\lambda_{ci} > 0$.

When the flow is incompressible, P is identically zero. The characteristic equation of velocity gradient tensor $\boldsymbol{A}$ reduces to $\lambda^3 + Q\lambda + R = 0$, so $p = Q$ and $q = R$. The expression for λ_{ci} is still,

$$\lambda_{ci} = \sqrt{3}(\zeta - \eta)/2, \tag{6}$$

but,

$$\lambda_r = \zeta + \eta, \tag{7a}$$

$$\lambda_{cr} = -(\zeta + \eta)/2, \tag{7b}$$

where

$$\zeta = \sqrt[3]{-R/2 + \sqrt{(R/2)^2 + (Q/3)^3}}, \tag{8a}$$

$$\eta = \sqrt[3]{-R/2 - \sqrt{(R/2)^2 + (Q/3)^3}}, \tag{8b}$$

and

$$R = -\det(\boldsymbol{A}), \tag{9a}$$

$$Q = 0.5\ \mathrm{tr}(-\boldsymbol{A}A). \tag{9b}$$

To illustrate the utility of the analytic solution, we now consider the effects of using either the total velocity field or the fluctuating field to identify vortex filaments. Both approaches have been used in the literature, and there is uncertainty concerning which is better. We consider first the general case of 3D, fully developed, incompressible turbulent flow and then the specific case of a Burgers vortex in a mean shear flow, the Burgers vortex representing the fluctuating flow.[6]

The (x, y, z) coordinates of the fully developed flow are taken to be the streamwise, wall-normal and spanwise directions, respectively, and the mean shear is $\partial U/\partial y$. The corresponding mean, fluctuating and total velocity components are (U, V, W), (u, v, w), and $(U(y) + u, v, w)$. Then, the gradient tensors of total and fluctuating velocity in 3D flow are

$$A_t = \begin{bmatrix} \frac{\partial u}{\partial x} & \frac{\partial (U+u)}{\partial y} & \frac{\partial u}{\partial z} \\ \frac{\partial v}{\partial x} & \frac{\partial v}{\partial y} & \frac{\partial v}{\partial z} \\ \frac{\partial w}{\partial x} & \frac{\partial w}{\partial y} & \frac{\partial w}{\partial z} \end{bmatrix}, \tag{10a}$$

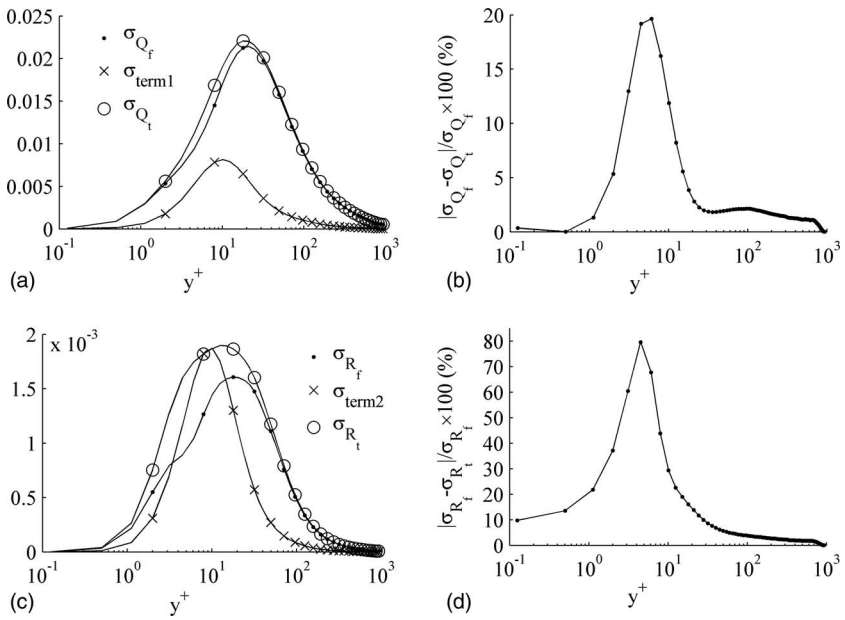

FIG. 1. Profiles of rms and relative deviations of the tensor invariant terms affected by mean shear. (a) RMS of Q_f, *term*1, and Q_t, normalized by $(\nu/u_\tau^2)^2$; (b) relative deviation between σ_{Q_f} and σ_{Q_t}; (c) rms of R_f, *term*2, and R_t, normalized by $(\nu/u_\tau^2)^3$; and (d) relative deviation between σ_{R_f} and σ_{R_t}.

$$A_f = \begin{bmatrix} \frac{\partial u}{\partial x} & \frac{\partial u}{\partial y} & \frac{\partial u}{\partial z} \\ \frac{\partial v}{\partial x} & \frac{\partial v}{\partial y} & \frac{\partial v}{\partial z} \\ \frac{\partial w}{\partial x} & \frac{\partial w}{\partial y} & \frac{\partial w}{\partial z} \end{bmatrix}. \tag{10b}$$

From Eq. (6), the algebraic solutions of 3D swirling strength can be calculated as

$$\begin{cases} \lambda_{ci,f} = \frac{\sqrt{3}}{2}\left[\sqrt[3]{-R_f/2+\sqrt{(R_f/2)^2+(Q_f/3)^3}} - \sqrt[3]{-R_f/2-\sqrt{(R_f/2)^2+(Q_f/3)^3}}\right] \\ \lambda_{ci,t} = \frac{\sqrt{3}}{2}\left[\sqrt[3]{-R_t/2+\sqrt{(R_t/2)^2+(Q_t/3)^3}} - \sqrt[3]{-R_t/2-\sqrt{(R_t/2)^2+(Q_t/3)^3}}\right] \end{cases}, \tag{11}$$

where $Q_f = 0.5\mathrm{tr}(-A_fA_f)$, $R_f = -\det(A_f)$, $Q_t = Q_f - \frac{\partial v}{\partial x}\frac{\partial U}{\partial y}$, and $R_t = R_f + \frac{\partial U}{\partial y}\left(\frac{\partial v}{\partial x}\frac{\partial w}{\partial z} - \frac{\partial v}{\partial z}\frac{\partial w}{\partial x}\right)$.

Hence, the mean shear influences the 3D swirling strength through

$$term1 = \frac{\partial \mathrm{v}}{\partial \mathrm{x}}\frac{\partial \mathrm{U}}{\partial \mathrm{y}} \text{ and } term2 = \frac{\partial U}{\partial y}\left(\frac{\partial v}{\partial x}\frac{\partial w}{\partial z} - \frac{\partial v}{\partial z}\frac{\partial w}{\partial x}\right),$$

and the magnitude of its effect will be significant, unless $\partial U/\partial y$ is much less than the fluctuating gradients. It will be shown later that this condition may or may not hold, depending on the local nature of the turbulent flow.

To quantitatively analyze the influence of mean shear on vortex detection by swirling strength, we must assess the relative magnitudes of Q_f, *term*1, Q_t, R_f, *term*2, and R_t, in a well-known and representative turbulent flow. The direct numerical simulation (DNS) of fully developed turbulent channel flow at friction Reynolds number $\mathrm{Re}_\tau = 934$ by Del Alamo *et al.*[7] is used for this purpose.

Since $\overline{term1}$ and $\overline{term2}$, averaged over time and homogeneous directions, vanish in fully developed flow, we measure the magnitudes of *term*1 and *term*2 by their root mean square (rms) values. Figures 1(a) and 1(c) show that the *rms* values of *term*1 and *term*2 are large enough to potentially influence vortex identification by swirling strength in the region $y^+ < 50$, where the mean shear is strongest. In Figure 1(a), the rms values σ_{Q_f} and σ_{Q_t} differ clearly in the domain $2 < y^+ < 30$; in Figure 1(c), the σ_{R_f} and σ_{R_t} differ in the domain $1 < y^+ < 50$. Relative deviations of these discrepancies are shown in Figures 1(b) and 1(d). The relative deviation between σ_{Q_f} and σ_{Q_t} is larger than 2% for $1 < y^+ < 30$, and the largest deviation reaches about 20%. Moreover, relative deviation between σ_{R_f} and σ_{R_t} is larger than 5% for $0.1 < y^+ < 50$, and the largest deviation reaches about 80%. It is concluded that mean shear influences vortex identification mainly in the region $y^+ < 50$, a layer slightly thicker than the buffer layer. In the outer region of the flow, the mean shear has little effect on vortex identification.

To assess the effects of mean shear on a well-known vortex, we consider the fluctuating velocity field (u, v, w) of a Burgers vortex rotating about the z-direction:

$$\begin{cases} (u, v) = -\dfrac{\alpha}{2}(x, y) + \dfrac{\Gamma}{2\pi}\left[1 - \exp\left(-\dfrac{x^2 + y^2}{4\nu/\alpha}\right)\right]\dfrac{1}{x^2 + y^2}(-y, x) \\ w = \alpha z \end{cases}. \tag{12}$$

Here, α is the strain-rate, ν is the kinematic viscosity, $r_0 = \sqrt{4\nu/\alpha}$ is the core radius (determined by the balance of viscous diffusion and strain), Γ is the circulation, and the spanwise vorticity ω_z at the vortex center is given by $\Gamma / \left(\pi r_o^2\right)$. If $\Gamma > 0$, the vortex rotates counter-clockwise.

Suppose that the flow field in (12) is imbedded in a background mean shear $\partial U/\partial y > 0$. In the parlance of turbulent vortices, a clockwise rotating Burgers vortex ($\Gamma > 0$) is called *retrograde*, because it rotates with the mean shear; a counter-clockwise rotating vortex ($\Gamma < 0$) is called *prograde*.[8] For purposes of illustration, it suffices to analyze the values of swirling strengths of the fluctuating and total velocity fields at the center of the Burgers vortex. They are

$$\lambda_{ci,f}(0,0,0) = \frac{\sqrt{3}}{2}\left(\sqrt[3]{f(\alpha) + \frac{|\Gamma|\left(\Gamma^2 + 144\pi^2\nu^2\right)}{\left(2\sqrt{3}\pi r_0^2\right)^3}} - \sqrt[3]{f(\alpha) - \frac{|\Gamma|\left(\Gamma^2 + 144\pi^2\nu^2\right)}{\left(2\sqrt{3}\pi r_0^2\right)^3}}\right), \tag{13a}$$

$$\lambda_{ci,t}(0,0,0) = \frac{\sqrt{3}}{2}\sqrt[3]{f(\alpha) - \left(\frac{\alpha}{2}\right)^2\frac{\Gamma}{4\pi\nu}\frac{\partial U}{\partial y} + g\left(\frac{\partial U}{\partial y}\right)\sqrt{\Gamma^2 - 2\pi r_0^2\frac{\partial U}{\partial y}\Gamma}}$$

$$-\frac{\sqrt{3}}{2}\sqrt[3]{f(\alpha) - \left(\frac{\alpha}{2}\right)^2\frac{\Gamma}{4\pi\nu}\frac{\partial U}{\partial y} - g\left(\frac{\partial U}{\partial y}\right)\sqrt{\Gamma^2 - 2\pi r_0^2\frac{\partial U}{\partial y}\Gamma}}, \tag{13b}$$

where

$$f(\alpha) = \left(\frac{\alpha}{2}\right)^3 + \frac{\alpha}{2}\left(\frac{\Gamma}{2\pi r_0^2}\right)^2 \tag{14}$$

and

$$g\left(\frac{\partial U}{\partial y}\right) = \left|\Gamma^2 + 144\pi^2\nu^2 - 2\pi r_0^2\Gamma\frac{\partial U}{\partial y}\right| \Big/ \left(2\sqrt{3}\pi r_0^2\right)^3. \tag{15}$$

By inspection of (13a), it is always true that

$$\lambda_{ci,f}(0,0,0) > 0,$$

so the fluctuating velocity gradient tensor can always successfully detect a prograde or retrograde Burgers vortex.

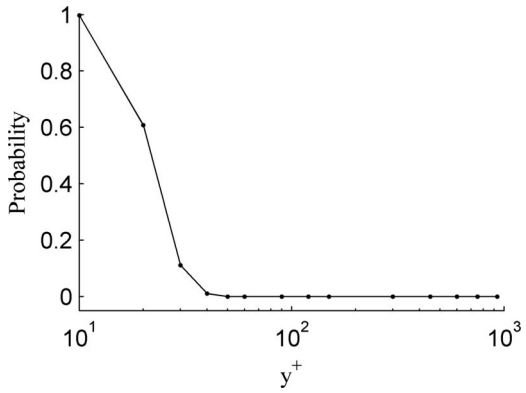

FIG. 2. Probability $P(\frac{\omega_z}{2}|_y < \frac{\partial U}{\partial y}(y))$ as a function of wall-normal position.

In the case of the total velocity field, if

$$term3 = \Gamma^2 - 2\pi r_0^2 \frac{\partial U}{\partial y}\Gamma > 0, \tag{16}$$

then (13b) implies

$$\lambda_{ci,t}(0, 0, 0) > 0,$$

and the swirling strength of the total field successfully indicates the presence of a Burgers vortex. For prograde vortices ($\Gamma < 0$), (16) is inherently positive, and $\lambda_{ci,t}(0, 0, 0)$ is always greater than zero, which means the mean shear has no influence on their identification. But, in the case of retrograde vortices ($\Gamma > 0$), when

$$\frac{\partial U}{\partial y} > \frac{\Gamma}{2\pi r_o^2}, \tag{17}$$

Term3 is negative and $\lambda_{ci,t}$ is complex, contradicting $\lambda_{ci} > 0$. Thus, when the background mean shear is greater than one-half of the vorticity ($\omega_z > 0$) at the center of a retrograde Burgers vortex, the total velocity gradient tensor will fail to identify it.

This result is disappointing, but it may or may not be an unphysical artifact of artificially summing a mean shear and an independent Burgers vortex. In real turbulence, the vortices and the mean flow are not really independent because vortices arise from instabilities of the base flow, and turbulent mean flow is likely the result of averaging over many eddies. Thus, the mean flow actually contains a contribution from the eddies, and the flow surrounding an eddy may not be accurately represented by the mean flow. Put another way, the fluctuating field found from Reynolds' Decomposition may not be a good representation of the eddies. This is a deep question that we will not attempt to solve here. Consequently, application of (17) to real turbulent shear flows is problematic, and it is, therefore, important to ask how often the mean shear might satisfy the inequality in (17) in real turbulence. To this end we have used the same DNS channel flow data to study the relation between $\partial U/\partial y$ and $\omega_z/2$ at the retrograde vortex centers. Unlike Wu and Christensen[8] and Herpin *et al.*,[9] the 3D swirling strength of the fluctuating velocity gradient tensor is used to extract vortex core centers, but the criterion $\lambda_{ci,f}(x, y, z) / \lambda_{ci,f}^{rms}(y) \geq 1.5$, where $\lambda_{ci,f}^{rms}(y)$ is the root mean square of $\lambda_{ci,f}$ at a given y position, is otherwise the same as theirs. Corresponding fluctuating velocity fields in x-y planes are used to calculate the fluctuating vorticity ω_z at retrograde vortex centers.

Cumulative distribution functions (CDFs) of $\omega_z/2$ at various wall-normal positions ($10 < y^+ < 930$) are calculated. Probability $P(\frac{\omega_z}{2}|_y < \frac{\partial U}{\partial y}(y))$ is defined as the ratio of the number of centers, at which half of the fluctuating vorticity is smaller than the mean shear, to the total sample number. Figure 2 presents the probability as a function of wall-normal position. It is obvious that probability is zero for $y^+ \geq 50$, which means in this region both total and fluctuating velocity gradient tensors can detect the original vortices. So there is no difference between results of these two methods for y^+

≥ 50. However, as y^+ decreases from 50 to 10, the probability increases dramatically approaching one at $y^+ = 10$. Hence, in the buffer layer a large proportion of retrograde spanwise vortices would not be detected by using the total velocity gradient tensor. Fortunately, quasi-streamwise vortices are believed to dominate the buffer layer.

In conclusion, this work presents new analytic solutions for the 3D swirling strength of compressible or incompressible flows. To illustrate the utility of these solutions, the difference between detecting vortices using the gradient tensors of either the fluctuating velocity or the total velocity was studied. A 3D Burgers vortex in a mean shear was used to study the difference, which depends on the strength of mean shear relative to the vorticity at the vortex center. Vortex detection always works well for prograde Burgers vortices, but for retrograde Burgers vortices the swirling strength fails to detect the vortex if the mean shear is greater than one-half of the maximum vorticity in the core. Data from DNS of channel flow at $\mathrm{Re}_\tau = 934$ show that the swirling strengths of the total versus the fluctuating field differ only for retrograde spanwise vortices in the region for $y^+ < 50$, which may explain the marked reduction in the density of retrograde vortices relative to prograde vortices near the wall.[8,9] Above this height, the λ_{ci} criterion is insensitive to using the fluctuating field or the total field. It should be noted that in consideration of the complexity of the full range of physical flows, the problem of which field is more appropriate for vortex identification in general merits further research.

This work was funded by National Natural Science Foundation of China (Grant No. 51127006) and the U. S. National Science Foundation under Grant No. CBET-0933848. H.C. also received financial support from the China Scholarship Council (CSC). We wish to acknowledge Professor R. D. Moser for supplying the channel DNS data, which were produced in conjunction with J. Jiménez, J.-C. Del Álamo, and P. S. Zandonade.

[1] J. C. R. Hunt, A. A. Wray, and P. Moin, "Eddies, streams, and convergence zones in turbulent flows," in *Proceedings of the Summer Program of the Center for Turbulence Research* (NASA Ames/Stanford University, USA, 1988), pp. 193–208.
[2] M. S. Chong, A. E. Perry, and B. J. Cantwell, "A general classification of three-dimensional flow fields," Phys. Fluids **2**(5), 765–777 (1990).
[3] J. Jeong and F. Hussain, "On the identification of a vortex," J. Fluid Mech. **285**, 69–94 (1995).
[4] J. Zhou, R. J. Adrian, S. Balachandar, and T. M. Kendall, "Mechanisms for generating coherent packets of hairpin vortices in channel flow," J. Fluid Mech. **387**, 353–396 (1999).
[5] N. Jacobson, *Basic Algebra I*, 2nd ed. (W. H. Freeman and Company, New York, 1985), pp. 264–266.
[6] The Burgers vortex is an Oseen vortex imbedded in an axisymmetric staining motion. Although the straining extends to infinity, it is treated as a local strain (i.e., fluctuating) when Burgers vortex is used to model a small vortex in larger scale turbulence.
[7] J. C. Del Álamo, J. Jiménez, P. Zandonade, and R. D. Moser, "Scaling of the energy spectra of turbulent channels," J. Fluid Mech. **500**, 135–144 (2004).
[8] Y. Wu and K. T. Christensen, "Population trends of spanwise vortices in wall turbulence," J. Fluid Mech. **568**, 55–76 (2006).
[9] S. Herpin, M. Stanislas, and J. Soria, "The organization of near-wall turbulence: A comparison between boundary layer SPIV data and channel flow DNS data," J. Turbul. **11**(47), 1–30 (2010).